

Dalton Transactions

Accepted Manuscript

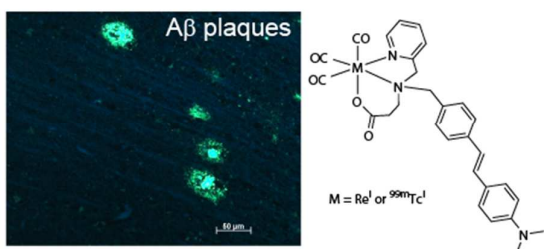


This is an *Accepted Manuscript*, which has been through the Royal Society of Chemistry peer review process and has been accepted for publication.

Accepted Manuscripts are published online shortly after acceptance, before technical editing, formatting and proof reading. Using this free service, authors can make their results available to the community, in citable form, before we publish the edited article. We will replace this *Accepted Manuscript* with the edited and formatted *Advance Article* as soon as it is available.

You can find more information about *Accepted Manuscripts* in the [Information for Authors](#).

Please note that technical editing may introduce minor changes to the text and/or graphics, which may alter content. The journal's standard [Terms & Conditions](#) and the [Ethical guidelines](#) still apply. In no event shall the Royal Society of Chemistry be held responsible for any errors or omissions in this *Accepted Manuscript* or any consequences arising from the use of any information it contains.



$[\text{M}(\text{CO})_3]^+$ (where M = Tc or Re) complexes with tridentate ligands featuring stilbene functional group have been prepared that bind to amyloid- β plaques that are a hallmark of Alzheimer's Disease.



Rhenium and Technetium Complexes that bind to Amyloid- β Plaques

David J. Hayne,^{a,b} Andrea J. North,^{a,b} Michelle Fodero-Tavoletti,^{c,e} Jonathan M. White,^{a,b} Lin W. Hung,^{b,c} Angela Rigopoulos,^f Catriona A. McLean,^{c,g} Paul A. Adlard,^c Uwe Ackermann,^e Henri Tochon-Danguy,^e Victor L. Villemagne,^{c,e} Kevin J. Barnham^{b,c,d} and Paul S. Donnelly^{*a,b}.

Alzheimer's disease is associated with the presence of insoluble protein deposits in the brain called amyloid plaques. The major constituent of these deposits is aggregated amyloid- β peptide. Technetium-99m complexes that bind to amyloid- β plaques could provide important diagnostic information on amyloid- β plaque burden using Single Photon Emission Computed Tomography (SPECT). Tridentate ligands with a stilbene functional group were used to form complexes with the *fac*-[M^I(CO)₃]⁺ (M = Re or ^{99m}Tc) core. The rhenium carbonyl complexes with tridentate co-ligands that included a stilbene functional group and a dimethylamino substituent bound to amyloid- β present in human frontal cortex brain tissue from subjects with Alzheimer's disease. This chemistry was extended to make the analogous [^{99m}Tc(CO)₃]⁺ complexes and the complexes were sufficiently stable in human serum. Whilst the lipophilicity ($\log D_{7.4}$) of the technetium complexes appeared ideally suited for penetration of the blood-brain barrier, preliminary biodistribution studies in an AD mouse model (APP/PS1) revealed relatively low brain uptake (0.24 %ID/g at 2 min post injection).

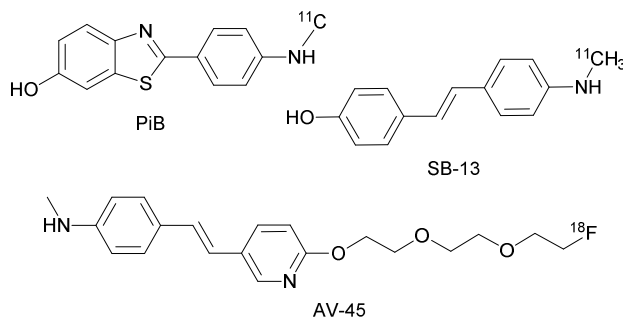
Introduction

Alzheimer's disease (AD) is the major cause of neurodegenerative dementia. A pathological hallmark of the disease is the presence of extracellular senile plaques in the brain. The major constituent of these plaques is an aggregated peptide called amyloid- β (A β), a 39-43 amino acid peptide derived from the amyloid precursor protein (APP).^{1,2} The exact role of A β plaques in dementia remains controversial, but extensive cortical A β deposition is a common feature identified by post-mortem analysis of AD subjects.³ Clinical diagnosis of AD relies on tests to establish progressive impairment of memory and in at least one other area of cognition.^{4,5} Molecular imaging techniques offer the possibility of identifying disease associated pathology and the desire for earlier and more accurate diagnosis of AD has led to the development of radioactive tracers designed to cross the blood-brain barrier and bind with some degree of selectivity to A β plaques.

The fluorescent dye Thioflavin-T that binds to A β plaques *in vitro* provided the structural inspiration for the development of several radiolabelled benzothiazole and stilbene compounds that have been used with considerable success to quantify plaque burden in human patients. It is thought that these molecules enter a hydrophobic pocket or channel and bind to the plaques by way of a combination of hydrophobic and π - π interactions. The benzothiazole, 2-(4-[¹¹C]methylaminophenyl)-6-hydroxybenzothiazole, known as Pittsburgh compound-B or [¹¹C]PiB (Figure 1), makes use of the short-lived positron-emitting isotope ¹¹C to enable diagnostic imaging using positron emission tomography (PET).⁶⁻⁸ There are some similarities in the chemical structure of benzothiazoles, such as PiB, and other plaque targeting groups such as stilbenes, in that they have conjugated aromatic ring systems and are relatively planar molecules. A variety of stilbene and styrylpyridine derivatives are excellent probes for A β plaques and a stilbene derivative radiolabelled with carbon-11 (4-*N*-methylamino-4'-hydroxystilbene), known as SB-13 (Figure 1), binds selectively to A β plaques.^{3,9,10} Preliminary studies of SB-13 in humans were promising and stimulated continued explorations of stilbene and styrylpyridine derivatives, as probes for A β plaques.^{3,11} The longer half-life of fluorine-18 when

compared to carbon-11 ($^{11}\text{C} = 20.4 \text{ min}$, $^{18}\text{F} = 109.7 \text{ min}$) encouraged efforts to develop stilbene¹² or styrylpyridine^{13, 14} derivatives radiolabelled with fluorine-18 culminating in the recent FDA approval of ^{18}F -AV45 (florbetapir) (Figure 1) to detect the presence of amyloid.^{3, 5, 15-17}

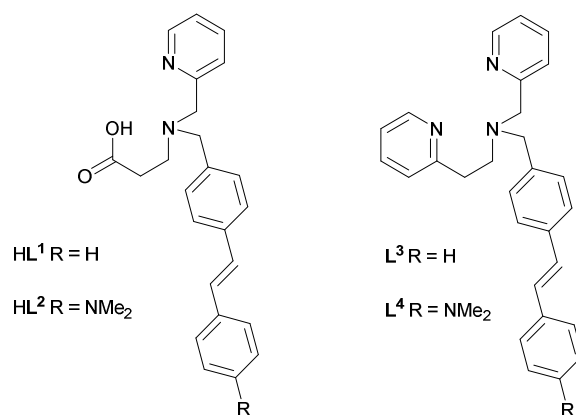
Figure 1: Chemical structures of [^{11}C]PiB, SB-13 and ^{18}F -AV45.



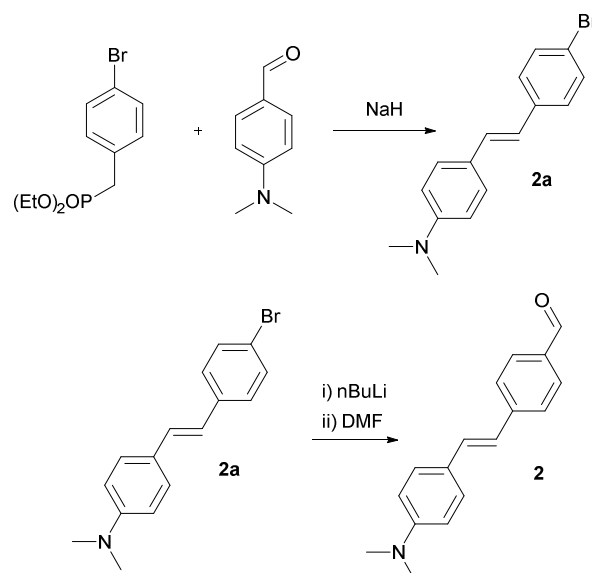
For imaging applications using carbon-11 or fluorine-18 radioisotopes the isotopes are produced by cyclotrons and the radionuclides are attached covalently to plaque binding molecules. Covalent attachment of radioisotopes to tracers requires complicated synthetic manipulations and specialist equipment. Despite the rapid increase in the number of hospitals equipped with the requisite infrastructure for PET, single photon emission computed tomography (SPECT) is the most commonly used nuclear imaging technique. The most commonly used radioisotope for SPECT is $^{99\text{m}}\text{Tc}$, which is available from convenient generators. The 6 hour half-life of $^{99\text{m}}\text{Tc}$ is sufficiently long to allow for the preparation of pure technetium complexes and for accumulation in target tissue, but short enough to not deliver excessive radiation doses to the patient. A $^{99\text{m}}\text{Tc}$ based radiotracer for determining plaque burden suitable for SPECT imaging would be of considerable clinical utility by increasing the number of centres that are able to perform diagnostic scans.¹⁸⁻²⁰ Several technetium complexes based on tetradentate N_2S_2 ligands fused to phenylbenzothiazole plaque binding groups designed to form neutral complexes with the $[\text{Tc}^{\text{V}}\text{O}]^{3+}$ have been synthesized. Some of these $[\text{Tc}^{\text{V}}\text{O}]^{3+}$ complexes show considerable promise and warrant further investigation.^{20, 21, 22} An alternative technetium 'core' to the $[\text{Tc}^{\text{V}}\text{O}]^{3+}$ is the low valent $[\text{Tc}^{\text{I}}(\text{CO})_3]^+$ and innovations in synthetic methodology have led to the possibility of preparing *fac*- $[\text{M}(\text{CO})_3(\text{H}_2\text{O})_3]^+$ (where $\text{M} = \text{Tc}^{\text{I}}$ or Re^{I}) using conditions amenable to radiopharmaceutical applications.²³⁻²⁵ The "carbonyl core" approach exploits the stability of the metal tricarbonyl core by substituting the water ligands with ligands designed to modify biodistribution. In the absence of non-radioactive isotopes of technetium the Group VII congener rhenium, which by virtue of the lanthanide contraction has similar ionic radii to technetium, is often used as a surrogate to guide synthetic developments. This manuscript describes the synthesis and characterisation of tridentate ligands designed to bind to the $[\text{M}(\text{CO})_3]^+$ core ($\text{M} = \text{Tc}^{\text{I}}/\text{Re}^{\text{I}}$) that feature pendent stilbene functional groups designed to bind to amyloid plaques. The ability of the new rhenium complexes to bind to $\text{A}\beta$ plaques in human brain tissue is assessed and the preliminary brain uptake of the $^{99\text{m}}\text{Tc}$ analogues is determined in both wild-type mice and a mouse model of $\text{A}\beta$ plaque pathology (APP/PS1).

Results and Discussion

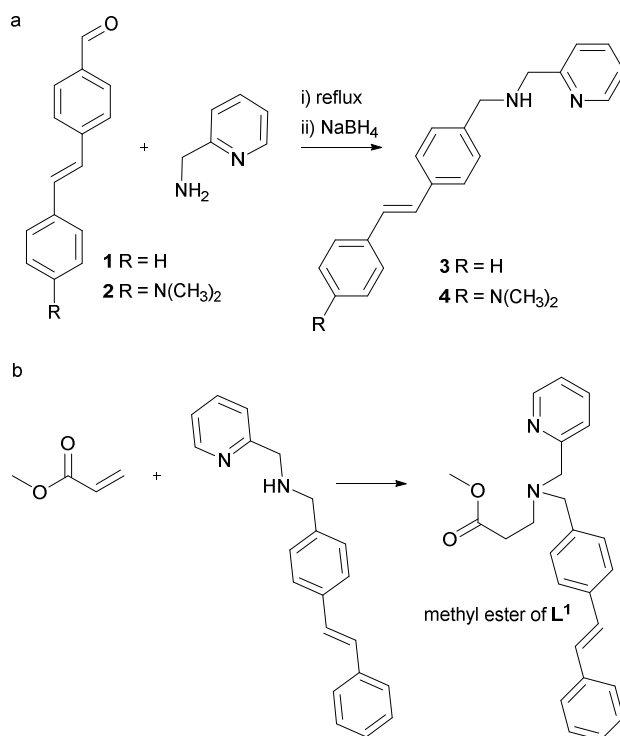
Synthesis and Characterisation. The *fac*- $[\text{M}(\text{CO})_3(\text{H}_2\text{O})_3]^+$ ($\text{M} = \text{Tc}^{\text{I}}/\text{Re}^{\text{I}}$) cation can be considered a "semi metal aqua cation" where the carbonyl ligands stabilize the low oxidation state and the *trans* effect increases the lability of coordinated water molecules. Ligands containing an aromatic amine and carboxylate donors coordinate to *fac*- $[\text{M}(\text{CO})_3]^+$ with rapid complexation kinetics producing complexes with good stability in aqueous solvents. Tridentate ligands bearing two pyridyl groups such as dipicolylamine serve as a versatile and useful starting point for bifunctional ligands where the amine nitrogen can be used to tether targeting groups. In this manuscript we present the synthesis of two pyridylamine-carboxylate tridentate ligands (HL^1 , HL^2) and two dipyridylamine ligands (L^3 , L^4) that each feature stilbene-like functional groups connected by a short alkyl linker (Figure 2).

Figure 2: Chemical structures of ligands H_2L^{1-2} and L^{3-4} 

The synthesis of the tridentate ligands HL^2 and L^4 utilised aldehyde **2**, (*E*)-4-(4-*N,N*-dimethylaminostyryl)benzaldehyde, that was prepared by formylation of *E*-4-(4-bromostyryl)-*N,N*-dimethylaniline (**2a**). Precursor **2a** was prepared by a Horner–Wadsworth–Emmons reaction between diethyl-4-bromobenzylphosphonate and 4-*N,N*-dimethylaminobenzaldehyde (Scheme 1). The methyl ester of L^1 was prepared by reductive amination of 2-picolyamine with *E*-4-stilbenecarboxaldehyde (**1**) to give pyridyl amine **3** followed by an aza-Michael addition with methyl acrylate (Scheme 2). The synthesis of L^3 involved aza-Michael addition between pyridyl amine **3** and 2-vinylpyridine. Reductive amination of aldehyde **2** with 2-picolyamine followed by aza-Michael additions with either methyl acrylate or 2-vinylpyridine furnished either the methyl ester of L^2 or L^4 (Scheme 2). The methyl esters of L^1 and L^2 , were hydrolysed to give the corresponding carboxylic acids, HL^1 and HL^2 .

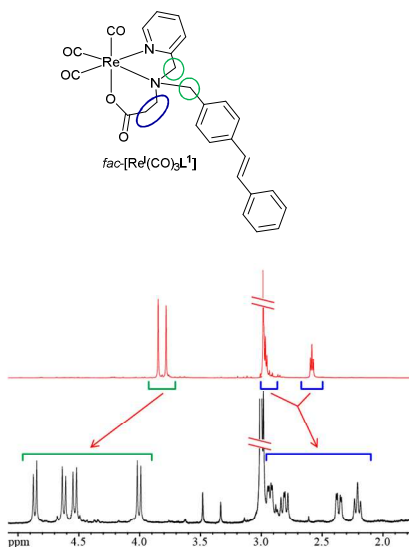
Scheme 1: Synthesis of precursor **2a** by Wadsworth-Emmons-Horner reaction followed by formylation of **2a** to give aldehyde **2**.

Scheme 2: a) Reductive amination of (*E*)-stilbene-carboxyaldehyde derivatives (aldehydes **1** or **2**) to give pyridylamines **3** or **4** respectively. b) Synthesis of proligand MeL¹ by aza-Michael addition of **3** with methyl acrylate.



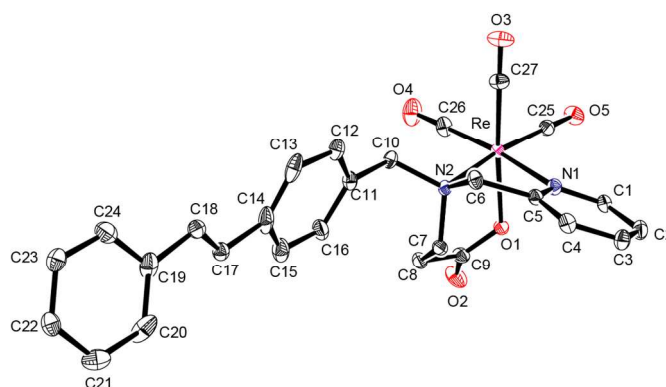
The rhenium complexes *fac*-[Re^I(CO)₃L¹⁻²] and *fac*-[Re^I(CO)₃L³⁻⁴]⁺ were prepared by microwave irradiation of an aqueous mixture of [Re^I(CO)₃(CF₃SO₃)] with the respective ligands in methanol. The use of microwave irradiation offers the advantage of high product yields with relatively short reaction times of about 30 minutes. For each complex, analysis by ¹H NMR spectroscopy confirmed the *E*-stereochemistry of the stilbene pendant groups was retained (³J_{HH} > 16 Hz). Upon coordination to the metal the methylene and ethylene protons of each ligand become diastereotopic, for example, the ¹H NMR spectrum of the methyl ester of L¹ has singlets for each of the two methylene groups and two multiplets for the proton pairs within the ethylene that split into in four AB doublets for each methylene proton and four multiplets for the ethylene protons upon coordination (Figure 2).

Figure 2: ¹H NMR spectra of MeL¹ (red) and *fac*-[Re^I(CO)₃L¹] (black). Methylene protons and signals are highlighted with green marks and ethylene with blue.



The crystal structures of $fac-[Re^I(CO)_3L^1]$ and $fac-[Re^I(CO)_3L^3]^+$ show distorted octahedral geometry about the metal centre with carbonyl groups arranged facially. Compound $fac-[Re^I(CO)_3L^1]$ crystallises in the triclinic space group $P\bar{1}$ (Figure 3). The asymmetric unit contains two neutral complexes and acetonitrile solvent molecules. In $fac-[Re^I(CO)_3L^1]$, the remaining coordination sphere of the metal is completed by an NNO donor atom set provided by the pyridyl nitrogen, tertiary amine and carboxylate groups of the ligand. The rhenium ion is in the equatorial plane defined by two carbonyl groups and the nitrogen donor atoms of the ligand with apical sites occupied by the remaining carbonyl group and carboxylate oxygen. Coordination of the ligand sees the formation of a five membered chelate ring containing two nitrogen donor atoms (N1, N2) and a methylene carbon (C6) and a six membered chelate ring that includes the two ethylene carbons (C7, C8), tertiary amine nitrogen (N2), and carboxylate oxygen (O1). The bond distances between rhenium and the two N donor atoms differ, with bond Re-N1 being 2.186(5) Å and Re-N2 2.262(5) Å in length. The Re-N1 bond length is within the range of similar $fac-[Re^I(CO)_3NNO]$ complexes but bonds Re-O1 and Re-N2 are slightly longer, at 2.142(4) Å and 2.262(5) Å, compared to 2.107-2.132 Å and 2.232-2.255 Å respectively for similar complexes.²⁶⁻³¹ This is possibly due to the inclusion of a six membered chelate ring instead of two five membered chelate rings seen in other complexes with the same donor atom set.

Figure 3: An ORTEP representation of $fac-[Re^I(CO)_3L^1]$ with 30% probability thermal ellipsoids, hydrogen atoms and solvent atoms omitted for clarity. Selected bond lengths (Å): Re-N1 2.186(5), Re-N2 2.262(5), Re-O1 2.142(4), Re-C25 1.927(7), Re-C26 1.913(7), Re-C27 1.928(7).



Compound $fac-[Re^I(CO)_3L^3]^+$ crystallises in the monoclinic space group $P2_1/c$ (Figure 4). The asymmetric unit contains one cationic complex with the asymmetric ligand forming both a five and six membered chelate ring upon coordination. Bond Re-N3 (2.162(5) Å) is within the range of other $fac-[Re^I(CO)_3]^+$ complexes containing two pyridyl groups and a tertiary amine (Re-N_{py} = 2.155-2.187 Å) but Re-N1 is longer (2.213(4) Å). This is again likely due to the six membered chelate ring with the bond Re-N2 (2.251(4) Å) also being longer relative to similar complexes (Re-N_{amine} 2.216-2.242 Å).^{26, 27, 32-36}

Figure 4: An ORTEP representation of $fac-[Re^I(CO)_3L^3]^+$ with 30% probability thermal ellipsoids, disordered counterions (OTf) were removed by a squeeze procedure and hydrogen atoms are omitted for clarity. Selected bond lengths (Å): Re-N1 2.213(4), Re-N2 2.251(4), Re-N3 2.162(5), Re-C29 1.919(5), Re-C30 1.905(5), Re-C31 1.922(6).

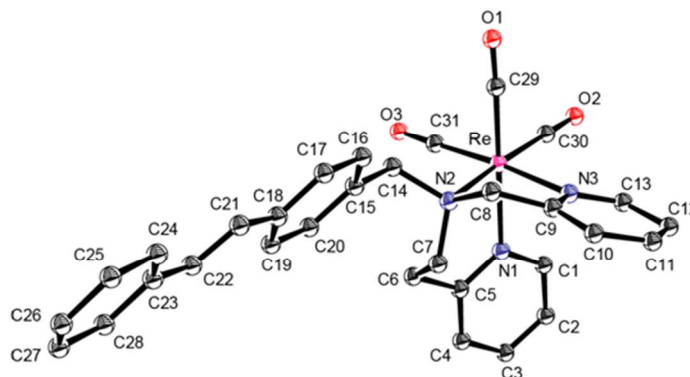
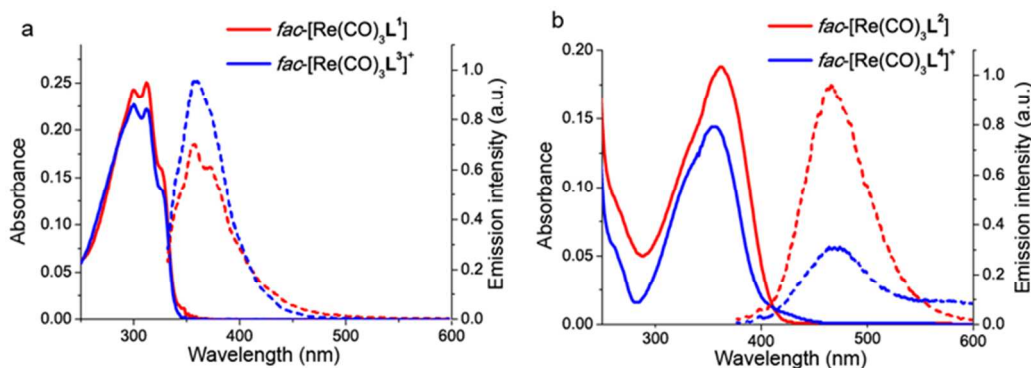


Table 1: Crystallographic Data for *fac*-[Re^I(CO)₃L¹] or *fac*-[Re^I(CO)₃L³]⁺.

	<i>fac</i> -[Re ^I (CO) ₃ L ¹]. 0.5MeCN	<i>fac</i> -[Re ^I (CO) ₃ L ³]CF ₃ SO ₃
Formula	C ₂₈ H _{24.50} N _{2.50} O ₅ Re	C ₃₂ H ₂₇ F ₃ N ₃ O ₆ ReS
<i>M</i>	662.20	824.82
Colour and Habit	Pink rod	Colourless block
Crystal size (mm ³)	0.13 × 0.06 × 0.04	0.36 × 0.27 × 0.21
System	Triclinic	Monoclinic
Space group	P $\bar{1}$	P 2 ₁ /c
T (°K)	130.0 K	130.0 K
<i>a</i> (Å)	10.6380(7)	13.3527(3)
<i>b</i> (Å)	12.5358(7)	14.7033(3)
<i>c</i> (Å)	19.0696(13)	17.0611(3)
α (°)	95.970(5)	90
β (°)	96.832(5)	91.244(2)
γ (°)	99.253(5)	90
<i>U</i> /Å ³	2472.4(3)	3348.79(12)
<i>Z</i>	4	4
<i>D</i> _{calcd} (Mg m ⁻³)	1.779	1.636
Wavelength (Å)	1.5418 (Cu-K α)	0.7107 (Mo-K α)
Absorption coefficient (mm ⁻¹)	9.980	3.754
F(000)	1300	1624
Reflections measured	17732	22309
Independent reflections	9825 [R _{int} = 0.0456]	7471 [R _{int} = 0.0272]
R [<i>I</i> > 2 σ (<i>I</i>)]	0.04	0.0378
wR(F ²) (all data)	0.0525	0.0509

Ligands HL¹⁻² and L³⁻⁴ are fluorescent due to the presence of the stilbene functional group. The methyl ester of L¹ and L³ have similar absorbance spectra each displaying two maxima at $\lambda_{\max} = 300$ nm and $\lambda_{\max} = 312$ nm. Both ligands fluoresce at $\lambda_{\text{em}} = 355$ nm following excitation at $\lambda_{\text{ex}} = 312$ nm. The absorbance spectra for *fac*-[Re^I(CO)₃L¹] and *fac*-[Re^I(CO)₃L³]⁺ have maxima at $\lambda_{\max} = 300$ and $\lambda_{\max} = 312$ nm, and an emission with a maximum at $\lambda_{\text{em}} = 360$ nm (Figure 5a). There is an increase in molar absorptivity upon coordination, from $27.0(\pm 0.2) \times 10^3 \text{ M}^{-1}\text{cm}^{-1}$ and $30.6(\pm 0.3) \times 10^3 \text{ M}^{-1}\text{cm}^{-1}$ for the methyl ester of L¹ and L³ respectively to $43.5(\pm 0.9) \times 10^3 \text{ M}^{-1}\text{cm}^{-1}$ for *fac*-[Re^I(CO)₃L¹] and $42.9(\pm 0.3) \times 10^3 \text{ M}^{-1}\text{cm}^{-1}$ for *fac*-[Re^I(CO)₃L³]⁺. The introduction of the electron donating dimethylamino functional group (HL² and L⁴) leads to a bathochromic shift of approximately 40 nm in the absorbance maxima (λ_{355} nm for HL², λ_{345} nm for HL⁴) and larger Stokes shifts of 90-100 nm. Complexes *fac*-[Re^I(CO)₃L²] and *fac*-[Re^I(CO)₃L⁴]⁺ are also fluorescent ($\lambda_{\text{em}} = 472$ nm for *fac*-[Re^I(CO)₃L²] and λ_{464} nm for *fac*-[Re^I(CO)₃L⁴]⁺ (Figure 5b)). The electronic spectra of stilbene and its derivatives are concentration dependent leading to excimer formation and stilbenes are photochromic but such detail was not investigated for these derivatives.

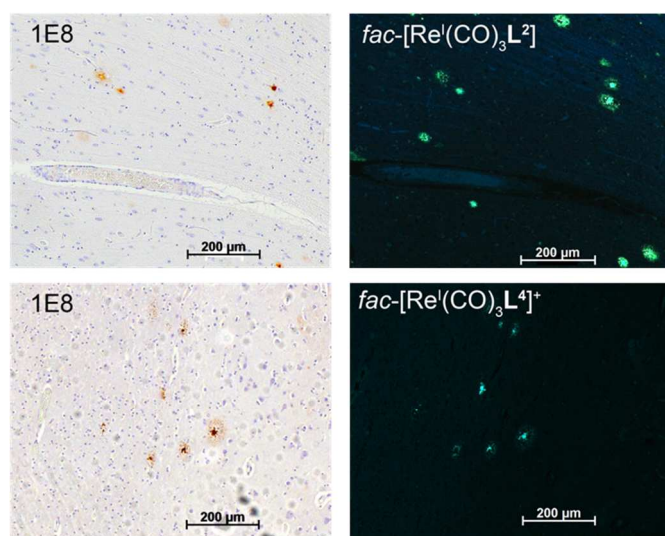
Figure 5: Absorbance (solid line) and emission (dotted line) spectra of a) *fac*-[Re^I(CO)₃L¹] (5 μM) and *fac*-[Re^I(CO)₃L³]⁺ (2 μM) in acetonitrile, $\lambda_{\text{ex}} = 312$ nm, and b) *fac*-[Re^I(CO)₃L²] (5 μM) and *fac*-[Re^I(CO)₃L⁴]⁺ (5 μM) in acetonitrile, $\lambda_{\text{ex}} = 355$ nm.



Binding of $fac-[Re^I(CO)_3L^{1-2}]$ & $fac-[Re^I(CO)_3L^{3-4}]^+$ to A β plaques in human brain tissue

Frontal cortex brain tissue collected from subjects with clinically diagnosed AD and age matched control subjects were used to determine the plaque-binding capacity of the new rhenium complexes. Amyloid- β plaques are typically 30-50 μ m in diameter so 5 μ m serial sections of tissue often contain comparable A β plaque distribution. A β plaques were stained with an A β antibody (1E8) and contiguous sections of brain tissue were treated with a solution of a chosen Re complex. The complexes $fac-[Re^I(CO)_3L^1]$ or $fac-[Re^I(CO)_3L^3]^+$ showed little to no plaque binding within brain tissue from AD positive subjects. The complexes that contained the electron-donating dimethylamino functional group were more promising. Epifluorescent microscopy of tissue sections treated with $fac-[Re^I(CO)_3L^2]$ and $fac-[Re^I(CO)_3L^4]^+$ reveal good correlation of the complexes to A β plaques stained with 1E8 antibody on the adjacent slide (Figure 6) especially with the plaque cores. Encouragingly there was no evidence of non-specific binding in the tissue from aged matched control subjects after treatment with $fac-[Re^I(CO)_3L^2]$ or $fac-[Re^I(CO)_3L^4]^+$ (see Supporting Information).

Figure 6.: Tissue sections from the frontal cortex of an AD affected brain (x10 magnification). Images on the left are immunohistologically stained using 1E8 antibody and viewed by bright-field microscopy. The matching adjacent slides treated with the rhenium complex and viewed by epifluorescence microscopy are on the right ($\lambda_{ex}=359$ nm, $\lambda_{em}=461$ nm).



Synthesis of $fac-[^{99m}Tc^I(CO)_3L^{1-2}]$ & $fac-[^{99m}Tc^I(CO)_3L^{3-4}]^+$.

Synthesis of technetium complexes, $fac-[^{99m}Tc^I(CO)_3L^{1-2}]$ and $fac-[^{99m}Tc^I(CO)_3L^{3-4}]^+$, involved addition of the tridentate ligands to $fac-[^{99m}Tc^I(CO)_3(H_2O)]^+$, adjustment of the reaction mixture to pH 6 and incubation of the mixture at 70°C for 20 min. The RP-HPLC profile of the technetium complexes was compared to the respective analogous rhenium complex. The slight difference in the retention times between the UV-Vis detection of the Re complexes and the radioactive peak of the technetium complexes is at least partially attributed to the configuration of the detectors. Both carboxylate containing ligands, HL¹ and HL², labelled with high radiochemical yield, affording $fac-[^{99m}Tc^I(CO)_3L^1]$ and $fac-[^{99m}Tc^I(CO)_3L^2]$ in >98% radiochemical purity without purification (Figure 7). A mixture of products was formed when reacting $fac-[^{99m}Tc^I(CO)_3(H_2O)]^+$ with the ligands containing two pyridyl functional groups, L³ and L⁴. Radiochemical purity of the desired complexes after incubation at 70 °C for 20 min was ~50% and ~40%, for $fac-[^{99m}Tc(CO)_3L^3]^+$ and $fac-[^{99m}Tc(CO)_3L^4]^+$ respectively. The complexes were found to be stable over several hours allowing sufficient time for purification by 'Sep-Pak' reverse phase C18 columns. The use of aqueous ethanol improved the radiochemical purity of $fac-[^{99m}Tc(CO)_3L^4]^+$ to 80%.

The lipophilicity of the complexes was estimated by measuring the partitioning of $fac-[^{99m}Tc^I(CO)_3L^{1-2}]$ and $fac-[^{99m}Tc^I(CO)_3L^{3-4}]^+$ between 1-octanol and PBS (pH 7.4) to give a $\log D_{7.4}$ value. It is difficult to predict if small molecules will be capable of crossing the blood-brain barrier but lipophilicity is an important criterion to be considered. Compounds with a $\log P$ of 1-3.5 are considered to have the best potential to cross the blood-brain barrier.³⁷ The $\log D_{7.4}$ values ranged from 1.0 for $fac-[^{99m}Tc^I(CO)_3L^4]^+$ to 2.1 for $fac-[^{99m}Tc^I(CO)_3L^1]$. The addition of the dimethylamino functional group results in complexes that are less lipophilic (Table 2).

Figure 7: Representative RP-HPLC trace of (a) $fac-[M(CO)_3L^1]$ (where $M = Re^I$, black; $M = {}^{99m}Tc^I$, red). Absorbance measured at 254 nm.

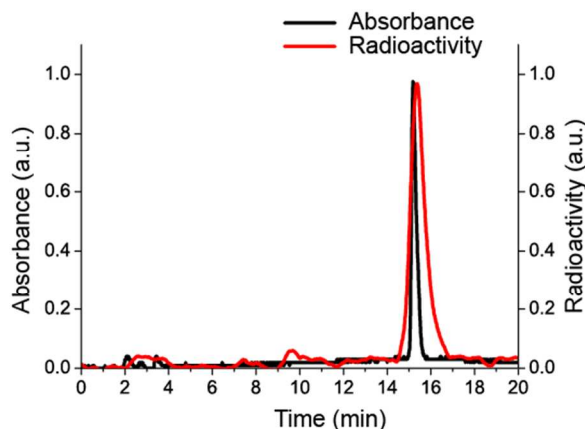


Table 2: $\text{Log}D_{7,4}$ values of $fac-[{}^{99m}Tc^I(CO)_3L^{1,2}]$ and $fac-[{}^{99m}Tc^I(CO)_3L^{3,4}]^+$.

	$fac-[{}^{99m}Tc^I(CO)_3L^1]$	$fac-[{}^{99m}Tc^I(CO)_3L^2]$	$fac-[{}^{99m}Tc^I(CO)_3L^3]^+$	$fac-[{}^{99m}Tc^I(CO)_3L^4]^+$
$\text{Log}D_{7,4}$	2.1	1.7	1.8	1.0

Stability of $fac-[{}^{99m}Tc^I(CO)_3L^2]$ & $fac-[{}^{99m}Tc^I(CO)_3L^4]^+$ in blood serum and in vivo biodistribution

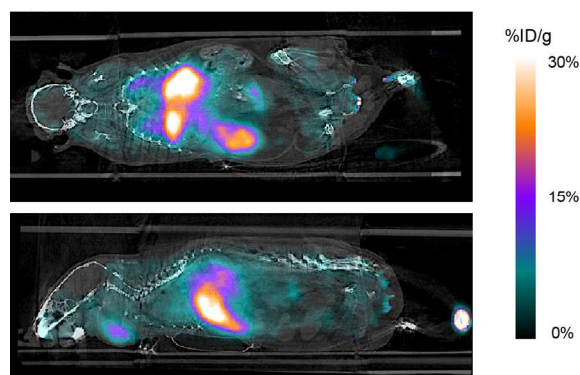
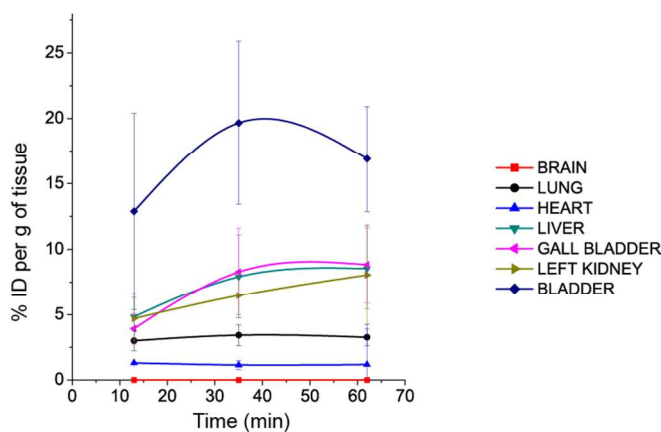
The complexes $fac-[Tc^I(CO)_3L^2]$ and $fac-[Tc^I(CO)_3L^4]^+$ were added to human sera and incubated at 37°C with aliquots of the mixture taken for analysis by RP-HPLC. Proteins were removed from by addition of acetonitrile to incipient precipitation followed by centrifugation and the supernatant was analysed by HPLC. The neutral complex, $fac-[{}^{99m}Tc^I(CO)_3L^1]$ remains stable in serum for over three hours but there is some degradation of the cationic complex, $fac-[{}^{99m}Tc^I(CO)_3L^4]^+$, evident after incubation in serum but the complex still retained ~60% radiochemical purity.

The biodistribution of $fac-[{}^{99m}Tc^I(CO)_3L^2]$ was investigated in both wild-type (WT) and 10 month old APP/PS1 transgenic mice. The APP/PS1 transgenic (Tg) amyloid model results in high A β plaque levels in the brain. The accumulation of radioactivity was predominately in the liver and kidneys. Brain uptake was detected at 2 min post injection (0.25% ID/g for WT and 0.24% ID/g for Tg) but with no statistically significant difference between wild-type and transgenic mice at either 2 minutes or 30 minutes post injection (mpi) (2 mpi, $p = 0.429$; 30 mpi, $p = 0.136$) (Table 3). An effective radiotracer for A β plaques would record higher radioactivity for brain tissue from the transgenic mice, particularly at 30 min post injection..

Micro-SPECT images of transgenic mice (3 \times APP/PS1) were acquired after administering $fac-[{}^{99m}Tc^I(CO)_3L^4]^+$ by intravenous tail injection with anatomical information afforded by X-ray computed tomography (CT). Post-mortem immunohistochemical staining of brain tissue samples confirmed the presence of A β plaques. Visual inspection of the co-registered SPECT/CT images reveal that activity due to accumulation of ${}^{99m}Tc$ is concentrated within the thoracic region with activity also detected in the abdomen and the thyroid (Figure 8). Retention of activity within the thyroid may indicate instability of the complex, $fac-[{}^{99m}Tc^I(CO)_3L^4]$, with respect to oxidation, resulting in formation of pertechnetate ($[{}^{99m}Tc^{VII}O_4]$).³⁸ No uptake is apparent in the cranial region indicating no or very low brain uptake of $fac-[{}^{99m}Tc^I(CO)_3L^4]^+$. A plot of activity over time confirms the lack of $fac-[{}^{99m}Tc^I(CO)_3L^4]^+$ uptake across the blood-brain barrier *in vivo* (Figure 9). The majority of activity was shown to be within the bladder. A large amount of activity was also recorded within the gall bladder and liver indicating excretion of the compound by both the urinary and hepatobiliary system.

Table 3: Biodistribution of $fac-[^{99m}Tc(CO)_3L^2]$ in APP/PS1 transgenic mice and wild-type-mice (n = 3); Average %dose/g (standard deviation).

	Wild-type		APP/PS1	
	2 min	30 min	2 min	30 min
	Ave (std)	Ave (std)	Avg (std)	Avg (std)
Blood	12.87 (3.82)	9.75 (0.43)	11.71 (0.62)	8.47 (1.04)
Brain	0.25 (0.05)	0.21 (0.02)	0.24 (0.02)	0.19 (0.01)
Liver	26.95 (7.84)	26.13 (4.69)	24.64 (5.70)	20.32 (0.65)
Spleen	7.88 (3.80)	8.97 (4.77)	6.67 (1.07)	5.96 (0.97)
Heart	5.43 (1.84)	4.25 (0.62)	5.25 (0.48)	3.59 (0.20)
Stomach	1.69 (0.81)	3.77 (0.70)	2.06 (0.93)	2.19 (1.68)
Kidney	25.32 (9.24)	19.60 (1.09)	24.76 (4.29)	18.45 (0.90)
Intestine	3.15 (0.91)	4.39 (1.71)	3.15 (1.02)	4.15 (0.59)

Figure 8: Coronal and sagittal co-register SPECT/CT images of an APP/PS1 transgenic mouse after intravenous tail injection of $fac-[^{99m}Tc(CO)_3L^4]^+$ (~3.5 MBq in 200 μ L of 10% ethanol in saline (0.9%)). Amount of radioactivity is shown by the scale bar on the right.**Figure 9:** Time activity plot of selected organs from transgenic mice administered $fac-[^{99m}Tc(CO)_3L^4]^+$. Activity was recorded at 13 min, 35 min and 62 min.

Conclusion

Four tridentate ligands designed to coordinate to $fac-[Re^I(CO)_3]^+$ and $fac-[^{99m}Tc^I(CO)_3]^+$ and bind to A β plaques *via* a stilbene functional group were synthesised. The rhenium complexes were characterised by a combination of NMR, electronic spectroscopy

and mass spectrometry, and two rhenium complexes were characterised by X-ray crystallography. The complexes with an electron-donating dimethylamino substituent on the stilbene functional group, *fac*-[Re^I(CO)₃L²] and *fac*-[Re^I(CO)₃L⁴]⁺, bound to Aβ plaques present in post-mortem brain tissue collected from human AD subjects. Analogous technetium complexes were prepared from [^{99m}Tc^{VII}O₄]⁻ using an 'Isolink' kit that uses potassium boranocarbonate as both a reducing agent and a source of carbon monoxide. The neutral complexes [^{99m}Tc^I(CO)₃L¹] and [^{99m}Tc^I(CO)₃L²] were more stable in human serum than the cationic complexes, [^{99m}Tc^I(CO)₃L³] and [^{99m}Tc^I(CO)₃L⁴] and all four technetium complexes have log*D*_{7.4} values that suggested appropriate lipophilicity for penetration of the blood-brain barrier *via* non-facilitated processes. Preliminary biodistribution and micro-SPECT imaging experiments revealed that although neutral [^{99m}Tc^I(CO)₃L²] displayed higher brain uptake than cationic [^{99m}Tc^I(CO)₃L⁴], the degree of brain uptake in a transgenic murine model of amyloid pathology was relatively low (0.24% ID/g). Effective penetration of the blood-brain barrier is a major challenge in the development of metal-based imaging agents designed to offer insight into the molecular aspects of neurodegeneration. Compounds that bind to Aβ plaques are often lipophilic and consequently display high levels of deposition in the lungs and liver and also susceptible to metabolism by P450 enzymes. Nonspecific binding to albumin and other serum proteins can also decrease the dose of a particular tracer that enters the brain. It would be of interest to investigate if these technetium complexes are substrates for either p-glycoprotein or breast cancer resistant protein, as both function as efflux pumps that act to remove substrates from the brain.^{39, 40, 41} The relative small size and low molecular weight of the [Tc^I(CO)₃]⁺ core makes it attractive for the synthesis of lipophilic and neutral molecules capable of crossing the blood-brain barrier and providing diagnostic information on Aβ plaque burden central to the progression of Alzheimer's disease. In this work tridentate ligands with a stilbene functional group were used to form complexes featuring the [Re^I(CO)₃]⁺ core that bound to Aβ plaques in human subjects. This chemistry was extended to make complexes based on [^{99m}Tc^I(CO)₃]⁺ and further investigations aimed at structural modifications for improving the brain uptake of these complexes is warranted.

Experimental

General synthetic chemistry procedures. All reagents and solvents were obtained from commercial sources and used as received unless otherwise stated. Microwave reactions were carried out using a Biotage Initiator microwave reactor. Nuclear magnetic spectra were acquired on an Agilent 400-MR (¹H NMR at 400 MHz and ¹³C{¹H} NMR at 101 MHz) or Varian FT-NMR 500 spectrometer (¹H NMR at 500 MHz and ¹³C{¹H} NMR at 126 MHz) at 298 K. All chemical shifts were referenced to the internal solvent residue and quoted in ppm relative to TMS. Chemical & MicroAnalytical Services Pty. Ltd., Victoria, Australia, carried out elemental analyses for C, H and N. Analytical radio-HPLC was performed using a Shimadzu 10AVP UV-Vis detector (Shimadzu, Kyoto, Japan), two LC-10ATVP solvent delivery systems (for solvent A (0.1% trifluoroacetic acid in MilliQ H₂O) & B (0.1% trifluoroacetic acid in acetonitrile)), a Nacalai Tesque Cosmosil 5C18-AR Waters column (4.6 mm I.D. × 150 mm) (Nacalai Tesque, Kyoto, Japan). The mobile phase used was a gradient consisting of 5% solvent B at t = 0 to 100% solvent B after 20 min. All runs were conducted at a constant total flow rate of 1 mL.min⁻¹ and the absorbance was monitored at λ 254 nm. The Re analogues of ^{99m}Tc complexes were used to confirm synthesis of complexes by comparison of retention times when analysed by RP-HPLC. Absorbance spectra were obtained on a Shimadzu UV-1650PC UV/visible spectrophotometer and emission spectra were obtained on a Varian CARY Eclipse fluorescence spectrometer, with both performed using capped quartz cuvettes. Infrared spectra were recorded using a Perkin-Elmer Spectrum One FTIR spectrometer, with a zinc selenide/diamond universal ATR 60 sampling accessory.

Crystals of compounds were mounted in low temperature oil then flash cooled. Intensity data were collected at 130 K on an X-ray diffractometer with CCD detector using either Cu-Kα (λ = 1.54184 Å) or Mo-Kα (λ = 0.71073 Å) radiation. Data were reduced and corrected for absorption.⁴² The structures were solved by direct methods and difference Fourier synthesis using the SHELX⁴³ suite of programs as implemented within the WINGX⁴⁴ software. Thermal ellipsoid plots were generated using ORTEP-3 software. In both structures *fac*-[Re(CO)₃L¹] and *fac*-[Re(CO)₃L³]CF₃SO₃ the *trans*-stilbene moiety was disordered with two orientations of the alkene occupying the same site in the crystal. This was refined as a two-site disorder model with occupancies of ca. 63:37 for *fac*-[Re(CO)₃L¹] and 73:27 for *fac*-[Re(CO)₃L³]CF₃SO₃, equivalent carbon-carbon bonds were restrained to have the same bond distances, and equivalent carbon atoms restrained to have similar thermal parameters. The triflate counter-ion of *fac*-[Re(CO)₃L¹]CF₃SO₃ was disordered and could not be modelled satisfactorily. The contributions from this counter-ion were removed using the squeeze procedure,⁴⁵ which calculated 232 electrons unaccounted for in the void volume of the unit cell. This is reasonably consistent with four triflate anions in the unit cell. *fac*-[Re^I(CO)₃L¹].0.5MeCN: CCDC 1025768. *fac*-[Re^I(CO)₃L³]CF₃SO₃: CCDC 1025769

(E)-4-(4-Bromostyryl)-N,N-dimethylaniline (2a). Modified from a literature procedure.⁴⁶ To a dry round bottom flask was added 4-bromobenzyl bromide (3.57 g, 14.2 mmol) and triethyl phosphite (7.5 mL, 43.1 mmol). The reaction mixture was heated at reflux for 2.5 h then unreacted triethyl phosphite was removed by evaporation under reduced pressure and the residue was used

without further purification. DMF (8 mL), sodium hydride (80% w/w, 1.01 g, 33.7 mmol) and 4-dimethylaminobenzaldehyde (2.10 g, 14.1 mmol) were added to the residue and the mixture was stirred at ambient temperature for 12 h. The reaction was quenched by the addition of ethanol then water to afford a green precipitate. The precipitate was collected by filtration, dissolved in dichloromethane (40 mL), washed with water (3x 40mL), and the organic phase was then dried (MgSO₄). The MgSO₄ was removed by filtration and petroleum spirits (boiling range 40-60°C) were added to the filtrate to give (*E*)-4-(4-bromostyryl)-*N,N*-dimethylaniline as yellow plate-like crystals (3.75 g, 12.4 mmol, 88%). ¹H NMR (400 MHz; CDCl₃): δ 7.43 (m, 4H, ArH), 7.34 (m, AA'BB', 2H, ArH), 7.03 (d, ³J_{HH} = 16.3, 1H, CH=CH), 6.84 (d, ³J_{HH} = 16.3, 1H, CH=CH), 6.72 (m, AA'BB' 2H, ArH), 2.99 (s, 6H, N(CH₃)₂). ESI-MS (+ve ion) [M+H]⁺ *m/z* 302.071 (experimental), 302.05 (calculated for C₁₆H₁₇BrN⁺).

4-(4-Dimethylamino)styrylbenzaldehyde (2). Modified from a literature procedure.⁴⁶ To anhydrous and deoxygenated THF (5 mL) was added (*E*)-4-(4-bromostyryl)-*N,N*-dimethylaniline (0.48mg, 1.6 mmol) and the mixture was cooled to -78°C. To the reaction mixture was added *n*-butyl lithium (1.2 M, 2 mL, 2.4 mmol) dropwise and then DMF (2.6 mL). The mixture was stirred for 3.5 h at -78°C and then the reaction was diluted with diethyl ether (1 mL) followed by water to afford a bright yellow precipitate. The reaction mixture was extracted with dichloromethane (150 mL), washed with brine (100 mL), then water (3x 100 mL), the organic phase was then dried (MgSO₄), filtered and the solvent removed by evaporation under reduced pressure to afford 4-(4-dimethylamino)styrylbenzaldehyde as an orange crystalline powder (0.32 mg, 1.3 mmol, 82%). ¹H NMR (400 MHz; CDCl₃): δ 7.43 (m, 4H), 7.33 (d, *J* = 8.4, 2H), 7.03 (d, ³J_{HH} = 16.3, 1H), 6.84 (d, ³J_{HH} = 16.3, 1H), 6.72 (m, 2H), 2.99 (s, 6H). ESI-MS (+ve ion) [M+H]⁺ *m/z* 252.155 (experimental), 252.14 (calculated).

(*E*)-1-(pyridin-2-yl)-*N*-(4-styrylbenzyl)methanamine (3). To anhydrous ethanol (80 mL) was added 2-picolyamine (1 mL, 9.7 mmol) and *trans*-4-stilbene-carboxyaldehyde (0.98 g, 4.7 mmol). The reaction mixture was heated at reflux under an atmosphere of N₂. After 30 min sodium borohydride (0.71 g, 19 mmol) was added in small portions and the reaction was heated at reflux again. After 6 hours at reflux the reaction was cooled to ambient temperature, the mixture was adjusted to pH 10 (1M NaOH) then to pH 7 (1M HCl). The reaction mixture was extracted with dichloromethane and the organic phase was washed (3 x 100 mL, H₂O). The organic phase was dried (MgSO₄), filtered, the solvent removed by evaporation under reduced pressure, and the residue was dried under vacuum to yield a colourless wax (1.3 g, 4.4 mmol, 93%). Calc. for C₂₁H₂₀N₂·0.75H₂O: C, 80.35; H, 6.90; N, 8.98. Found: C, 80.4; H, 6.7; N, 8.9. ¹H NMR (500 MHz; CDCl₃): δ 8.62 (d, *J* = 4.7, 1H), 7.68 (m, 1H, PyH), 7.57-7.52 (m, 4H, ArH), 7.41-7.35 (m, 5H, ArH, PyH), 7.30 (m, 1H, ArH), 7.21 (m, 1H, PyH), 7.15 (s, 2H, CH=CH), 3.99 (s, 2H, CH₂), 3.90 (s, 2H, CH₂), 2.27 (s, 1H, NH). {¹H} ¹³C NMR (126 MHz; CDCl₃): δ 159.8, 149.4, 139.83, 137.5, 136.5, 136.2, 128.8, 128.7, 128.6, 128.4, 127.6, 126.7, 126.6, 122.5, 122.0, 54.6, 53.3. ESI-MS (+ve ion) *m/z* [M+H]⁺:301.170 (experimental), 301.17 (calculated for C₂₁H₂₁N₂⁺).

(*E*)-*N,N*-dimethyl-4-(4-((pyridin-2-ylmethylamino)methyl)styryl)aniline (4). To anhydrous ethanol (50 mL) was added 2-picolyamine (0.44 g, 9.7 mmol) and **2** (0.36 g, 1.4 mmol). The reaction mixture was set stirring and heated at reflux. After 1 h, sodium borohydride (0.70 g, 18.5mmol) was added in small portions and the reaction was heated at reflux again. After 6 hours, the reaction was cooled to ambient temperature and the mixture was adjusted to pH 12 (1 M NaOH) and then pH 7 (1M HCl). After extracting the reaction mixture with ethyl acetate the organic layer was washed with brine (2 x 100 mL), and then with water (3 x 100 mL), dried over MgSO₄, filtered and the solvent was evaporated under reduced pressure. The resultant waxy yellow residue was triturated with petroleum benzene (boiling range 40-60%) and isolated by filtration followed by purification by silica chromatography (chloroform) to afford compound **4** as a yellow powder (0.33 g, 0.97 mmol, 68%). Calc. for C₂₃H₂₅N₃·0.5H₂O: C, 78.37; H, 7.44; N, 11.92. Found: C, 78.7; H, 7.30; N, 12.10. ¹H NMR (500 MHz; CDCl₃): δ 8.57 (m, 1H, pyH), 7.64 (m, 1H, PyH), 7.45-7.40 (m, 5H), 7.32 (m, 3H, PyH, ArH), 7.17-7.15 (m, 1H, PyH), 7.03 (d, ³J_{HH} = 16.2, 1H, CH=CH), 6.91 (d, ³J_{HH} = 16.3, 1H, CH=CH), 6.72 (m, 2H, ArH), 3.94 (s, 2H, CH₂), 3.84 (s, 2H, CH₂), 2.98 (s, 6H, N(CH₃)₂). {¹H} ¹³C NMR (126 MHz; CDCl₃): δ 160.0, 150.2, 149.5, 138.8, 137.2, 136.5, 128.7, 128.6, 127.7, 126.2, 126.0, 124.4, 122.5, 122.0, 112.6, 54.7, 53.4, 40.6. ESI-MS (+ve ion) [M+Na]⁺ *m/z* 344.212, (experimental), 344.21 (calculated for C₂₃H₂₆N₃⁺).

(*E*)-methyl 3-((pyridin-2-ylmethyl)(4-styrylbenzyl)amino)propanoate (methyl ester of L¹). To ethanol (30 mL) was added **3** (0.40 g, 1.3 mmol), methyl acrylate (0.25 mL, 2.8 mmol) and acetic acid (0.20 mL, 3.5 mmol). The mixture was heated at reflux for 26 hr then cooled to ambient temperature and the solvent was removed by evaporation under reduced pressure. The crude product was eluted through a plug of silica using ethyl acetate, the solvent removed and the residue dried *in vacuo* to afford the methyl ester of L¹ as a yellow oil (0.32 g, 0.83 mmol, 62%). Calc. for C₂₅H₂₆N₂O₂: C, 77.69; H, 6.78; N, 7.25. Found: C, 77.5; H, 6.7; N, 7.2. ¹H NMR (500 MHz; CDCl₃): δ 8.51 (ddd, ³J_{HH} = 4.9, ⁴J_{HH} = 1.8, ⁵J_{HH} 0.9 Hz, 1H, PyH), 7.66 (m, 1H, PyH), 7.52-7.49 (m, 3H, ArH), 7.47-7.45 (m, 2H, ArH), 7.37-7.32 (m, 4H, ArH), 7.25 (m, 1H, PyH), 7.15 (ddd, ³J_{HH} = 7.4, ³J_{HH} = 4.9, ³J_{HH} = 1.2 Hz, 1H, PyH), 7.09 (s, 2H, CH=CH), 3.77 (s, 2H, CH₂), 3.65 (s, 2H, CH₂), 3.63 (s, 3H, CH₃), 2.88 (t, ³J_{HH} = 7.1 Hz, 2H, CH₂-CH₂), 2.54 (t, ³J_{HH} = 7.1 Hz, 2H, CH₂-CH₂). {¹H} ¹³C (126 MHz; CDCl₃): δ 173.0, 159.9, 149.0, 138.6, 137.5, 136.5, 136.4,

129.3, 128.8, 128.6, 128.5, 127.7, 126.6, 126.6, 123.0, 122.1, 60.0, 58.3, 51.6, 49.7, 32.8. ESI-MS (+ve ion) m/z [M+H]⁺ 387.211 (experimental), 387.21 (calculated for C₂₅H₂₆N₂O₂⁺).

(E)-methyl 3-((4-(4-(dimethylamino)styryl)benzyl)(pyridine-2-ylmethyl)amino)propanoate (methyl ester of L²). To ethanol (10 mL) was added **4** (0.40 g, 1.3 mmol), methyl acrylate (0.25 mL, 2.8 mmol) and acetic acid (0.20 mL, 3.5 mmol). The reaction mixture was shielded from light and stirred at ambient temperature under nitrogen atmosphere. After 48 h, the solvent and unreacted methyl acrylate were removed *in vacuo* to afford the methyl ester of L² as a yellow oil. (0.32 g, 0.74 mmol, 98%). ¹H NMR (400 MHz; CDCl₃): δ 8.50 (m, 1H, PyH), 7.65 (m, 1H, PyH), 7.49 (d, ³J_{HH} = 7.9, 1H, PyH), 7.43-7.39 (m, 4H, ArH), 7.29 (m, AA'BB', 2H, ArH), 7.14 (ddd, ³J_{HH} = 7.4, ³J_{HH} = 4.9, ⁴J_{HH} = 1.0, 1H, PyH), 7.02 (d, ³J_{HH} = 16.3, 1H, CH=CH), 6.89 (d, ³J_{HH} = 16.3, 1H, CH=CH), 6.71 (m, AA'BB', 2H, ArH), 3.76 (s, 2H, CH₂), 3.62 (s, 2H), 2.98 (s, 6H, N(CH₃)₂), 2.87 (t, ³J_{HH} = 7.1, 2H, CH₂), 2.53 (t, ³J_{HH} = 7.1, 2H, CH₂). ESI-MS (+ve ion) [M+H]⁺ m/z 430.259 (experimental), 430.25 (calculated for C₂₇H₃₂N₃O₂⁺).

(E)-3-((4-(4-(dimethylamino)styryl)benzyl) (pyridine-2-ylmethyl)amino)propanoic acid (HL²). To a mixture of methanol and distilled water (1:1, 14 mL) was added the methyl ester of L² (0.25 g, 0.58 mmol), CsCO₃ (.40 g, 1.1 mmol) and the reaction mixture was set stirring and heated at reflux for 1 h. The reaction mixture was then extracted into dichloromethane by gradual addition of HCl to the aqueous layer. The organic phase was dried (MgSO₄) and the solvent removed by evaporation under reduced pressure to afford HL² as a light yellow powder (0.16 g, 0.39 mmol, 67 %). Calc. for C₂₆H₂₉N₃O₂·H₂O: C, 72.03; H, 7.21; N, 9.69. Found: C, 72.0; H, 6.8; N, 9.7. ¹H NMR (500 MHz; CDCl₃): δ 8.59 (m, 1H, PyH), 7.67 (m, 1H, PyH), 7.43 (m, 4H, ArH), 7.26 (m, AA'BB', 2H, ArH), 7.23 (m, 2H, PyH), 7.04 (d, ³J_{HH} = 16.3, 1H, CH₂=CH₂), 6.88 (d, ³J_{HH} = 16.3, 1H, CH₂=CH₂), 6.71 (m, AA'BB', 2H, ArH), 3.85 (s, 2H, CH₂), 3.78 (s, 2H, CH₂), 2.97 (m, 8H, CH₂, N(CH₃)₂), 2.58 (t, ³J_{HH} = 6.2, 2H, CH₂). ¹³C NMR (126 MHz; CDCl₃): δ 173.6, 156.5, 150.3, 149.3, 138.2, 137.2, 133.9, 130.0, 129.4, 127.8, 126.4, 125.7, 123.8, 123.7, 122.9, 58.1, 57.8, 49.3, 40.6, 31.1. ESI-MS (+ve ion) [M+H]⁺ m/z 416.234 (experimental), 416.23 (calculated for C₂₆H₃₀N₃O₂⁺).

(E)-2-(pyridin-2-yl)-N-(pyridin-2-ylmethyl)-N-(4-styrylbenzyl)ethanamine (L³). To ethanol (40 mL) was added 2-vinylpyridine (0.35 mL, 3.2 mmol), **3** (0.48 g, 1.6 mmol) and acetic acid (0.40 mL, 7.0 mmol). The reaction mixture was heated at reflux for 36 h. The crude product was loaded onto a plug of silica and washed with 10% ethyl acetate in dichloromethane, 10% MeOH in ethyl acetate then eluted using 15% MeOH in ethyl acetate. The solvent was removed by evaporation under reduced pressure and the residue dried to afford L³ as a colourless wax (within crude: 0.39 g, 0.96 mmol, 99%). Calc. for C₂₀H₁₇N₃·0.5H₂O: C, 77.90; H, 5.88; N, 13.63. Found: C, 77.5; H, 5.8; N, 13.9. ¹H NMR (500 MHz; CDCl₃): δ 8.49 (m, 2H, PyH), 7.57 (m, 2H, PyH), 7.50 (m, 2H, ArH), 7.42 (m, AA'BB', 2H), 7.36 (m, 3H), 7.28 (m, AA'BB', 2H), 7.27 (m, 1H, PyH), 7.10 (m, 5H, PyH, CH=CH), 3.82 (s, 2H, CH₂), 3.71 (s, 2H, CH₂), 3.04 (m, 2H, CH₂-CH₂), 2.95 (m, 2H, CH₂-CH₂). ¹³C NMR (126 MHz; CDCl₃): δ 160.5, 159.9, 149.1, 148.8, 138.7, 137.5, 136.6, 136.4, 129.3, 128.8, 128.8, 128.6, 128.5, 127.7, 126.6, 126.5, 123.6, 123.0, 122.1, 121.3, 59.9, 58.4, 54.1, 359. ESI-MS (+ve ion) m/z [M+H]⁺ 406.228 (experimental), 406.23 (calculated for C₂₈H₂₈N₃⁺).

(E)-N,N-dimethyl-4-(((2-(pyridin-2-yl)ethyl)(pyridin-2-ylmethyl)amino)methyl)styryl)aniline (L⁴). To ethanol (10 mL) was added **4** (0.31 g, 0.90 mmol), 2-vinylpyridine (0.25 mL, 2.3 mmol) and acetic acid (0.25 mL, 4.4 mmol). The reaction mixture was shielded from light and stirred at ambient temperature under nitrogen atmosphere for 11 days, the solvent and excess 2-vinylpyridine were removed under reduced pressure to afford L⁴ as a yellow oil, (0.38 g, 0.74 mmol, 97%), which was purified by silica chromatography (CHCl₃/CH₃OH). Calc. for C₃₀H₃₂N₄·0.5H₂O: C, 78.74; H, 7.37; N, 12.24. Found: C, 79.0; H, 7.3; N, 12.2. ¹H NMR (500 MHz; CDCl₃): δ 8.48 (m, 2H, PyH), 7.56 (m, 2H, PyH), 7.42-7.38 (m, 4H, ArH), 7.36 (m, 2H, PyH), 7.25 (m, AA'BB', 2H, ArH), 7.09 (m, 2H, PyH), 7.01 (d, ³J_{HH} = 16.3, 1H), 6.89 (d, ³J_{HH} = 16.3, 1H), 6.70 (m, AA'BB', 2H), 3.82 (s, 2H, CH₂), 3.70 (s, 2H, CH₂), 2.98 (m, 10H, CH₂-CH₂, N(CH₃)₂). ¹³C NMR (126 MHz; CDCl₃): δ 160.8, 160.4, 150.2, 149.3, 148.9, 138.0, 137.0, 136.4, 136.2, 129.2, 128.5, 127.6, 126.0, 126.0, 124.4, 123.5, 122.9, 121.9, 121.2, 112.6, 60.2, 58.4, 54.2, 40.6, 36.2. ESI-MS (+ve ion) [M+H]⁺ m/z 449.283 (experimental), 449.27 (Calculated).

fac-[Re^I(CO)₃L¹]. To aqueous NaOH (1M, 3 mL) was added the methyl ester of L¹ (40 mg, 0.10 mmol). The reaction mixture was heated at reflux for 30 min then the mixture was allowed to cool to ambient and transferred to a microwave reaction flask. Methanol (7 mL) and [Re^I(CO)₅OTf] (51 mg, 0.11 mmol) were added and the pH adjusted to ~pH 7 by addition of HCl (1M). The flask was capped and irradiated at 150 °C (3 × 10 min) shaking between each heating cycle. The solvent volume was reduced by evaporation under a stream of nitrogen until the point of turbidity. The flask was sealed and stored at 4°C for 2 days and colourless crystals were observed. The solvent was decanted and the crystals washed with H₂O and dried *in vacuo* to afford fac-[Re^I(CO)₃L¹] as a colourless crystalline powder (40 mg, 0.062 mmol, 57%). Calc. for C₂₇H₂₃N₂O₅Re: C, 50.54; H, 3.61; N, 4.37. Found: C, 50.52; H, 3.67; N, 4.30. (thin film) ν (CO) 2017 cm⁻¹, 1903 cm⁻¹, 1873 cm⁻¹. ¹H NMR (500 MHz; CDCl₃): δ 8.92 (m, 1H, PyH), 7.93 (m, 1H, PyH), 7.62 (m, AA'BB', 2H, ArH), 7.54 (m, AA'BB', 2H, ArH), 7.47 (m, 1H, PyH), 7.39 (m, 3H, PyH, ArH), 7.32 (m, 3H, ArH), 7.20 (d, ³J_{HH} = 16.4 Hz, 1H, CH=CH), 7.13 (d, ³J_{HH} = 16.3 Hz, 1H, CH=CH), 4.88 (m, AB, 1H, CH₂), 4.65 (m, AB,

1H, CH₂), 4.56 (m, AB, 1H, CH₂), 4.02 (m, AB, 1H, CH₂), 2.92 (m, 1H, CH₂-CH₂), 2.82 (m, 1H, CH₂-CH₂), 2.41 (m, 1H, CH₂-CH₂), 2.23 (m, 1H, CH₂-CH₂). ¹H} ¹³C NMR (126 MHz; CDCl₃): δ 197.2, 195.9, 194.1, 177.2, 158.7, 153.8, 139.8, 139.2, 136.8, 132.5, 130.9, 129.5, 129.0, 128.4, 127.3, 127.1, 126.9, 126.2, 123.2, 66.9, 66.0, 49.8, 33.5. ESI-MS (+ve ion) [M+H]⁺ *m/z* 643.108 (experimental), 643.12 (calculated for C₂₇H₂₄N₂O₅Re⁺). Crystals suitable for X-ray diffraction were grown by evaporation of a solution of the complex dissolved in acetonitrile. IR

fac-[Re^I(CO)₃L²]. To a microwave reaction flask equipped with a stirrer bar was added [Re^I(CO)₅OTf] (41 mg, 0.10 mmol), and methanol (2.5 mL). The reaction flask was sealed and the mixture was heated to 150°C using MW irradiation (2 × 15 min). L² (42 mg, 0.10 mmol) was added to the reaction mixture and the MW vessel was sealed and irradiated to 150°C (15 min) then at 130°C (10 min). A precipitate was formed upon reducing the solvent volume under a stream of nitrogen. The precipitate was isolated by filtration to afford *fac*-[Re^I(CO)₃L²] as a yellow powder (30 mg, 0.44 mmol, 44%). IR ν(CO) 2021 cm⁻¹, 1906 cm⁻¹, 1886 cm⁻¹. Calc. for C₂₉H₂₈N₃O₅Re.2.5H₂O: C, 47.73; H, 4.56; N, 5.76. Found: C, 47.8; H, 4.5; N, 5.7. ¹H NMR (500 MHz; CDCl₃): δ 8.93 (m, 1H, PyH), 7.92 (m, 1H, PyH), 7.56 (m, AA'BB', 2H, ArH), 7.43 (m, 4H, ArH, PyH), 7.29 (m, AA'BB', 2H, ArH), 7.13 (d, ³J_{HH} = 16.3, 1H, CH=CH), 6.92 (d, ³J_{HH} = 16.3, 1H, CH=CH), 6.74-6.72 (m, AA'BB', 2H, PyH), 4.87 (m, AB, 1H, CH₂), 4.63 (m, AB, 1H, CH₂), 4.54 (m, AB, 1H, CHH), 4.01 (m, AB, 1H, CHH), 3.01 (s, 6H, N(CH₃)₂), 2.93 (m, 1H, CHH-CH₂), 2.82 (m, 1H, CH₂-CHH), 2.37 (m, 1H, CH₂-CHH), 2.22 (m, 1H, CHH-CH₂). ¹H} ¹³C NMR (126 MHz; CDCl₃): δ 197.2, 195.9, 194.2, 177.3, 158.8, 153.7, 150.7, 140.1, 139.7, 132.4, 131.0, 128.3, 128.0, 126.5, 126.1, 125.1, 123.2, 122.7, 112.5, 66.9, 66.0, 49.7, 40.5, 33.5. ESI-MS(+ve ion) [M+H]⁺ *m/z* 686.164 (experimental), 686.17 (calculated for C₂₉H₂₉N₃O₅Re).

fac-[Re^I(CO)₃L³]CF₃SO₃. A microwave reaction flask was charged with L³ (50 mg, 0.11 mmol), [Re^I(CO)₅OTf] (43 mg, 1.1 mmol) and methanol (3 mL). The flask was capped and the reaction mixture was irradiated at 150°C (3 × 10 min), shaking between each heating cycle. To the mixture was added diethyl ether and colourless crystals were observed. The reaction mixture was stored at -18°C overnight and the resultant crystals were isolated by filtration to afford *fac*-[Re^I(CO)₃L³]CF₃SO₃ as colourless crystals (63 mg, 0.074 mmol, 70%). Calc. for C₃₂H₂₇F₃N₃O₆ReSN₃.H₂O: C, 45.60; H, 3.47; N, 4.99. Found: C, 45.7; H, 3.3; N, 4.6. IR ν(CO) 2027 cm⁻¹, 1901 cm⁻¹, 1869 cm⁻¹. ¹H-NMR (500 MHz; CDCl₃): δ 9.03 (m, 1H, pyH), 8.92 (m, 1H, PyH), 7.93 (m, 1H, PyH), 7.86 (m, 1H, PyH), 7.67 (m, 3H, PyH, ArH), 7.52 (m, 4H, ArH, PyH), 7.45 (m, 2H, ArH), 7.39 (m, 3H, ArH, PyH), 7.30 (m, 1H, PyH), 7.20 (d, ³J_{HH} = 16.4 Hz, 1H, CH=CH), 7.13 (d, ³J_{HH} = 16.3 Hz, 1H, CH=CH), 4.86 (m, AB, 1H, CHH), 4.71 (m, AB, 1H, CHH), 4.57 (m, AB, 1H, CHH), 4.43 (m, AB, 1H, CHH), 3.31 (m, 3H, CH₂-CHH), 2.19 (m, 1H, CH₂-CHH). ¹H} ¹³C NMR (126 MHz; CD₃OD): δ 196.8, 194.9, 194.5, 164.4, 161.5, 156.6, 153.4, 142.0, 141.8, 140.5, 138.4, 134.0, 131.5, 131.2, 129.8, 129.1, 128.5, 128.0, 127.9, 127.7, 127.6, 126.2, 125.7, 121.8 (q), 68.1, 67.9, 51.8, 35.6. ESI-MS (+ve ion) *m/z* [M]⁺ 676.159 (experimental), 676.16 (calculated). Crystals suitable for X-ray diffraction were grown by exchange of vapours between *n*-pentane and a solution of the complex in dichloromethane.

fac-[Re^I(CO)₃L⁴]CF₃SO₃. To a microwave reaction flask equipped with a stirrer bar was added [Re^I(CO)₅OTf] (40 mg, 0.080 mmol), L⁴ (40 mg, 0.090 mmol), and methanol (5 mL). The reaction vessel was sealed and the mixture was heated to 130°C using microwave irradiation (15 min) followed by further irradiation to 140°C (15 min). The solvent volume was reduced under a stream of nitrogen and diethyl ether (5 mL) was added, and the mixture was stored at -18°C for 12 h. The precipitate that formed was collected by filtration to afford *fac*-[Re^I(CO)₃L⁴]CF₃SO₃ as a yellow powder (15 mg, 0.017 mmol, 21%). Calc. for C₃₄H₃₂N₄F₃O₆ReS: C, 47.05; H, 3.72; N, 6.46. Found: C, 47.4; H, 3.7; N, 6.4. IR ν(CO) 2020 cm⁻¹, 1903 cm⁻¹, 1882 cm⁻¹. ¹H NMR (500 MHz; CDCl₃): δ 9.04 (m, 1H, PyH), 8.91 (m, 1H, PyH), 7.96 (m, 1H, PyH), 7.87 (m, 1H, PyH), 7.65 (m, 1H, PyH), 7.59 (m, AA'BB', 2H, ArH), 7.52 (m, 2H, PyH), 7.43 (m, 5H, ArH, PyH), 7.12 (d, ³J_{HH} = 16.2 Hz, 1H, CH=CH), 6.92 (d, ³J_{HH} = 16.3 Hz, 1H, CH=CH), 6.75 (m, AA'BB', 2H, ArH), 4.84 (m, AB, 1H, CHH), 4.69 (m, AB, 1H, CHH), 4.55 (m, AB, 1H, CHH), 4.38 (m, AB, 1H, CHH), 3.29 (m, 3H, CH₂-CHH), 3.01 (s, 6H, N(CH₃)₂), 2.19 (m, 1H, CH₂-CHH). ¹H} ¹³C NMR (126 MHz; CDCl₃): δ 195.8, 193.7, 193.5, 162.4, 159.4, 154.9, 151.8, 150.4, 141.3, 140.7, 140.4, 132.6, 131.0, 128.1, 127.9, 127.5, 127.0, 126.8, 125.5, 125.2, 123.0, 112.7, 67.7, 66.9, 51.3, 40.7, 34.8. ESI-MS(+ve ion) [M]⁺ *m/z* 719.199 (experimental), 719.20 (calculated for C₃₃H₃₃N₄O₃Re⁺).

Staining of human brain tissue

The Health Sciences Human Ethics Sub-committee, The University of Melbourne, approved all experiments using human brain tissue (Ethics Approval No. 1341145). Brain tissue was collected at autopsy. Brain tissue from the frontal cortex was preserved by formalin fixation and paraffin embedding. AD pathology was confirmed according to standard National Institute of Aging and Reagan Institute Working Group on Diagnostic Criteria for the Neuropathological Assessment of Alzheimer's Disease (1997) criteria. The brain tissue samples of age-matched Human control (HC) were subject to the above criteria. Deparaffinization of AD and HC sections (5µm) was carried out (xylene, 3 × 2min) prior to rehydration (soaked for 2 min in 100%, 90%, 70%, then 0% ethanol/water v/v). The slides were then washed in PBS (5min) and the autofluorescence was quenched with potassium permanganate (0.25% in PBS, 20 min) before washing again with PBS (2 × 20min). Samples were then treated with a solution of

potassium metabisulfite and oxalic acid (1% each in PBS) until the tissue changed from brown in colour to colourless then washed in PBS (3 × 2 min). The sections were blocked with bovine serum albumin (2% BSA in PBS, pH 7.4, 10 min) then treated covered with filtered compound (50 μM, 15% DMSO/PBS, 60 min). The sections were treated with BSA to remove any non-specifically bound complex and washed in PBS (3 × 2 min), then distilled water and finally mounted with non-fluorescent mounting media (Dako). Images were obtained on a Leica (Bannockburn, IL) DM1RB microscope fitted with a Carl Zeiss AxioCam MR colour camera.

Radiochemistry

General synthesis of $[\text{}^{99\text{m}}\text{Tc}^{\text{I}}(\text{CO})_3\text{L}^{1-4}]^+$ complexes. The $\text{fac-}[\text{}^{99\text{m}}\text{Tc}^{\text{I}}(\text{CO})_3(\text{H}_2\text{O})]^+$ starting material was prepared as directed by the manufacturer instructions supplied with the Isolink™ kit (Covidien). In short, $[\text{Tc}^{\text{VI}}\text{O}_4]^-$ (1000 MBq, in 0.9 % saline solution (1 mL)) eluted from a Gentech® generator was added to an Isolink™ kit (Mallinckrodt Medical B.V., The Netherlands) and was heated in a bath of boiling water. After 20 min, the kit was removed from the bath, let cool to ambient temperature and aliquots from the kit, containing $\text{fac-}[\text{}^{99\text{m}}\text{Tc}^{\text{I}}(\text{CO})_3(\text{H}_2\text{O})_3]^+$, was used for subsequent $^{99\text{m}}\text{Tc}$ labelling of ligands. The radiolabeling of ligands was carried out by addition of $\text{fac-}[\text{}^{99\text{m}}\text{Tc}^{\text{I}}(\text{CO})_3(\text{H}_2\text{O})_3]^+$ (100 μL) to a solution of the chosen ligand in dimethyl sulfoxide or ethanol (100 μL, 1 mg/mL). The reaction mixture was then adjusted to pH 6 by addition of 1M HCl and incubated at 70°C for 20 min.

Measurement of $\text{Log}D_{7.4}$ values. To a vial containing 1-octanol (5mL) and PBS (5 mL, 20 mM, pH 7.4) was added the radiotracer (50 μL). The mixture was shaken by hand for 3 min and the fractions were allowed to separate. The 1-octanol layer used in the subsequent steps and each measurement was carried out in triplicate. An aliquot of the 1-octanol layer (900 μL) was added to PBS (900 μL, 20 mM, pH 7.4). The two phases were mixed by mechanical shaking (5min) then separated by centrifuge (5 min at 13200 rpm, Eppendorf 5415 D centrifuge). A 500 μL aliquot of the organic phase and 500 μL from the aqueous phase was taken. The radioactive decay of each aliquot was measured in counts per minute (cpm) (Perkin-Elmer, Wizard 1470 automatic gamma counter) enabling calculation of the partition coefficient (D) and $\text{log}D_{7.4}$.

In vivo biodistribution of $\text{fac-}[\text{}^{99\text{m}}\text{Tc}^{\text{I}}(\text{CO})_3\text{L}^2]$ in mice.

All methods conformed to the Australian National Health and Medical Research Council published code of practice for animal research and The Howard Florey Animal Ethics Committee approved experimentation. All mice were housed according to standard animal care protocols and fed standard laboratory chow and tap water *ad libitum*. Mice were kept on a 12:12 hour light dark cycle and all testing was performed during the light phase of the circadian cycle. All studies were conducted in a blinded fashion.

A DMSO/saline solution (4.8% DMSO, 100μL volume per dose) of $[\text{}^{99\text{m}}\text{Tc}^{\text{I}}(\text{CO})_3\text{L}^2]$ (57 kBq) was injected directly into the tail vein of wild type and APP/PS1 transgenic mice. The mice were euthanized at either 2 or 30 min by intraperitoneal injection of sodium pentobarbitone (80 mg per kg) followed by perfusion with PBS and collection of the brain and other organs. The organs of interest were removed, weighed and the radioactive decay was measured in cpm (Packard Cobra II automatic gamma counter). The percentage dose per organ was calculated by comparison of the tissue counts with aliquots of the injected material.

SPECT/CT imaging of APP/PS1 transgenic mice after injection of $\text{fac-}[\text{}^{99\text{m}}\text{Tc}^{\text{I}}(\text{CO})_3\text{L}^4]^+$. To an Isolink™ kit (Mallinckrodt Medical B.V., The Netherlands) was added pertechnetate (1200 MBq in 1 mL 0.9% saline) and the mixture was heated at 100°C (20 min) affording $\text{fac-}[\text{}^{99\text{m}}\text{Tc}^{\text{I}}(\text{CO})_3(\text{H}_2\text{O})_3]^+$. To an Eppendorf™ tube was added L^4 (150 μL of L^4 in ethanol, 1 mg/mL), saline (0.9%, 352 μL), 1M HCl (10 μL) and $\text{fac-}[\text{}^{99\text{m}}\text{Tc}^{\text{I}}(\text{CO})_3(\text{H}_2\text{O})_3]^+$ (58 μL) and the mixture was heated at 70°C for 10 min affording $\text{fac-}[\text{}^{99\text{m}}\text{Tc}^{\text{I}}(\text{CO})_3\text{L}^4]^+$. Saline (0.9%, 1140 μL) was added to reduce the concentration of ethanol in the reaction mixture to 10%. The radiotracer, $\text{fac-}[\text{}^{99\text{m}}\text{Tc}^{\text{I}}(\text{CO})_3\text{L}^4]^+$, was administered to APP/PS1 transgenic mice (× 3, 15 months old, ~40 g) by intravenous tail injection (200 μL, 10% ethanol, specific activity 168 GBq/mmol). Acquisition of images using a SPECT/CT scanner (Mediso nanoScan SPECT/CT) was accomplished by 3 × 10 min static SPECT scans at approximately 2, 25 and 50 min post injection with one CT scan (25 kVp, 0.45 s, 0.99 mA, helical scan with 720 projections). To confirm the presence of Aβ plaques, brain tissue samples were immunohistochemically stained *ex vivo*, using 1E8 antibody.

Notes and references

Acknowledgements

The Australian Research Council is acknowledged for financial support. Covidien Ltd. provided the 'Isolink' kits used in this research. Dr Nouria Salehi (Royal Melbourne Hospital, Melbourne, Australia) is acknowledged for assistance in analysing biodistribution data. The Victorian Brain Bank is acknowledged for the provision of the brain tissue used in this study.

^a School of Chemistry, University of Melbourne, Melbourne, 3010, Australia

^b Bio21 Molecular Science and Biotechnology Institute, 30 Flemington Road The University of Melbourne Victoria 3010 Australia.

^c Florey Institute of Neuroscience and Mental Health, University of Melbourne, Parkville, Melbourne, Victoria, 3010, Australia.

^d Department of Pharmacology, University of Melbourne, Parkville, Melbourne, Victoria, 3010, Australia.

^e Department of Molecular Imaging and Therapy, Austin Health, Melbourne, Heidelberg, Victoria 3084, Australia.

^f Ludwig Institute for Cancer Research, Heidelberg, Victoria, Australia,

^g Department of Anatomical Pathology, The Alfred Hospital, Victoria 3181, Australia

† Footnotes should appear here. These might include comments relevant to but not central to the matter under discussion, limited experimental and spectral data, and crystallographic data.

Electronic Supplementary Information (ESI) available: Images of tissue sections from the frontal cortex of an age-matched control brain treated with $[\text{Re}(\text{CO})_3\text{L}^2]$ and $[\text{Re}(\text{CO})_3\text{L}^4]$. See DOI: 10.1039/b000000x/

- 1 C. L. Masters, G. Simms, N. A. Weinman, G. Multhaupt, B. L. McDonald and K. Beyreuther, *Proc. Nat. Acad. Sci. (USA)*, 1985, **82**, 4245.
- 2 J. A. Hardy and G. A. Higgins, *Science*, 1992, **256**, 184.
- 3 H. F. Kung, S. R. Choi, W. Qu, W. Zhang and D. Skovronsky, *J. Med. Chem.*, 2010, **53**, 933.
- 4 E. Karran, M. Mercken and B. De Strooper, *Nat. Rev. Drug Discov.*, 2011, **10**, 698.
- 5 C. C. Rowe and V. L. Villemagne, *J. Nucl. Med.*, 2011, **52**, 1733.
- 6 C. A. Mathis, Y. Wang, D. P. Holt, G.-F. Huang, M. L. Debnath and W. E. Klunk, *J. Med. Chem.*, 2003, **46**, 2740.
- 7 W. Zhang, S. Oya, M.-P. Kung, C. Hou, D. L. Maier and H. F. Kung, *Nucl. Med. Biol.*, 2005, **32**, 799.
- 8 R. Vandenberghe, K. Van Laere, A. Ivanoiu, E. Salmon, C. Bastin, E. Triau, S. Hasselbalch, I. Law, A. Andersen, A. Korner, L. Minthon, G. Garraux, N. Nelissen, G. Bormans, C. Buckley, R. Owenius, L. Thurfjell, G. Farrar and J. Brooks David, *Ann. Neurol.*, 2010, **68**, 319.
- 9 H. F. Kung, C.-W. Lee, Z.-P. Zhuang, M.-P. Kung, C. Hou and K. Ploessl, *J. Am. Chem. Soc.*, 2001, **123**, 12740.
- 10 M. Ono, A. Wilson, J. Nobrega, D. Westaway, P. Verhoeff, Z.-P. Zhuang, M.-P. Kung and H. F. Kung, *Nucl. Med. Biol.*, 2003, **30**, 565.
- 11 P. L. G. Verhoeff Nicolaas, A. Wilson Alan, S. Takeshita, L. Trop, D. Hussey, K. Singh, F. Kung Hank, M.-P. Kung and S. Houle, *Am. J. Geriatr. Psychiatry*, 2004, **12**, 584.
- 12 W. Zhang, S. Oya, M.-P. Kung, C. Hou, D. L. Maier and H. F. Kung, *J. Med. Chem.*, 2005, **48**, 5980.
- 13 W. Qu, M.-P. Kung, C. Hou, T. E. Benedum and H. F. Kung, *J. Med. Chem.*, 2007, **50**, 2157.
- 14 W. Zhang, M.-P. Kung, S. Oya, C. Hou and H. F. Kung, *Nucl. Med. Biol.*, 2007, **34**, 89.
- 15 S. R. Choi, G. Golding, Z. Zhuang, W. Zhang, N. Lim, F. Hefti, T. E. Benedum, M. R. Kilbourn, D. Skovronsky and H. F. Kung, *J. Nucl. Med.*, 2009, **50**, 1887.
- 16 L. Yang, D. Rieves and C. Ganley, *New Engl. J. Med.*, 2012, **367**, 885.
- 17 C. M. Clark, M. J. Pontecorvo, T. G. Beach, B. J. Bedell, R. E. Coleman, P. M. Doraiswamy, A. S. Fleisher, E. M. Reiman, M. N. Sabbagh, C. H. Sadowsky, J. A. Schneider, A. Arora, A. P. Carpenter, M. L. Flitter, A. D. Joshi, M. J. Krautkramer, M. Lu, M. A. Mintun and D. M. Skovronsky, *Lancet Neurol.*, 2012, **11**, 669.
- 18 M. Ono and H. Saji, *Int. J. Mol. Imaging*, 2011, 543267.
- 19 Z. Li, M. Cui, J. Dai, X. Wang, P. Yu, Y. Yang, J. Jia, H. Fu, M. Ono, H. Jia, H. Saji and B. Liu, *J. Med. Chem.*, 2013, **56**, 471.
- 20 J. L. Hickey and P. S. Donnelly, *Coord Chem Rev*, 2012, **256**, 2367.
- 21 D. J. Hayne, S. Lim and P. S. Donnelly, *Chem. Soc. Rev.*, 2014.
- 22 X. Chen, P. Yu, L. Zhang and B. Liu, *Bioorg. Med. Chem. Lett.*, 2008, **18**, 1442.
- 23 R. Alberto, R. Schibli, P. A. Schubiger, U. Abram and T. A. Kaden, *Polyhedron*, 1996, **15**, 1079.
- 24 R. Alberto, K. Ortner, N. Wheatley, R. Schibli and A. P. Schubiger, *J. Am. Chem. Soc.*, 2001, **123**, 3135.
- 25 R. Alberto, R. Schibli, R. Waibel, U. Abram and A. P. Schubiger, *Coord. Chem. Rev.*, 1999, **190-192**, 901.
- 26 Y. Mikata, K. Takahashi, Y. Noguchi, M. Naemura, A. Ugai, S. Itami, K. Yasuda, S. Tamotsu, T. Matsuo and T. Storr, *Eur. J. Inorg. Chem.*, 2012, **2012**, 217.
- 27 S. R. Banerjee, M. K. Levadala, N. Lazarova, L. Wei, J. F. Valliant, K. A. Stephenson, J. W. Babich, K. P. Maresca and J. Zubieta, *Inorg. Chem.*, 2002, **41**, 6417.
- 28 C. Dumas, J. Petrig, L. Frei, B. Spingler and R. Schibli, *Bioconjugate Chem.*, 2005, **16**, 421.
- 29 N. Marti, B. Spingler, F. Breher and R. Schibli, *Inorg. Chem.*, 2005, **44**, 6082.
- 30 J. Giglio, G. Patsis, I. Pirmettis, M. Papadopoulos, C. Raptopoulou, M. Pelecanou, E. Leon, M. Gonzalez, H. Cerecetto and A. Rey, *Eur. J. Med. Chem.*, 2008, **43**, 741.
- 31 A. Chiotellis, C. Tsoukalas, M. Pelecanou, C. Raptopoulou, A. Terzis, M. Papadopoulos, Z. Papadopolou-Daifoti and I. Pirmettis, *Inorg. Chem.*, 2008, **47**, 2601.
- 32 M. Patra, G. Gasser, D. Bobukhov, K. Merz, A. V. Shtemenko and N. Metzler-Nolte, *Dalton Trans.*, 2010, **39**, 5617.
- 33 L. A. Mullice, R. H. Laye, L. P. Harding, N. J. Buurma and S. J. A. Pope, *New J. Chem.*, 2008, **32**, 2140.
- 34 P. W. Causey, T. R. Besanger, P. Schaffer and J. F. Valliant, *Inorg. Chem.*, 2008, **47**, 8213.
- 35 S. R. Banerjee, J. W. Babich and J. Zubieta, *Inorg. Chem. Commun.*, 2004, **7**, 481.

- 36 S. R. Banerjee and J. Zubieta, *Acta Crystallogr., Sect. C Cryst. Struct. Commun.*, 2005, **C61**, m275.
- 37 D. D. Dischino, M. J. Welch, M. R. Kilbourn and M. E. Raichle, *J. Nucl. Med.*, 1983, **24**, 1030.
- 38 J. Meller and W. Becker, *Eur. J. Nucl. Med. Mol. Imaging*, 2002, **29 Suppl 2**, 38.
- 39 G. Lee and R. Bendayan, *Pharm. Res.*, 2004, **21**, 1313.
- 40 S. A. Hitchcock, *J. Med. Chem.*, 2012, **55**, 4877.
- 41 P. Kannan, V. W. Pike, C. Halldin, O. Langer, M. M. Gottesman, R. B. Innis and M. D. Hall, *Mol. Pharmaceutics*, 2013, **10**, 2222.
- 42 CrysAlis CCD, O. D. L. Version 1.171.32.5 (release 08-05-2007 CrysAlis171.NET; compiled May 8 2007,13:10:02).
- 43 G. M. Sheldrick, *Acta Crystallogr., Sect. A Found. Crystallogr.*, 2008, **64**, 112.
- 44 L. J. Farrugia, *J. Appl. Crystallogr.*, 1999, **32**, 837.
- 45 P. van der Sluis and A. L. Spek, *Acta Cryst. Sect. A*. 1990, 46, 194.
- 46 J. Sutharsan, M. Dakanali, C. C. Capule, M. A. Haidekker, J. Yang and E. A. Theodorakis, *ChemMedChem*, 2010, **5**, 56.